SF2A 2006
D. Barret, F. Casoli, T. Contini, G. Lagache, A. Lecavelier, and L. Pagani (eds)

GAMMA-RAY BINARIES, A NEW CLASS OF VERY HIGH ENERGY SOURCES

G. Dubus[1]

Abstract. There are now three sources of γ-rays with energies >100 GeV that have been identified with binaries in our galaxy: LS 5039, LS I+61 303 and PSR B1259-63. All are composed of a massive star and a compact object, neutron star or black hole. The interaction of the relativistic wind from a young pulsar with the stellar wind of the companion provides a common scenario to explain the emission from these sources. They join plerionic sources as the new stars of the VHE sky currently being uncovered by HESS.

1 Introduction

The new generation of Cherenkov telescopes HESS and MAGIC have increased the number of know TeV sources to more than 40, many of which are in the Galactic plane. Three of the Galactic sources have been associated with binary stars on the basis of their positional coincidence, variability and spectra: PSR B1259-63 (Aharonian et al., 2005b), LS 5039 (Aharonian et al., 2005a) and LS I +61°303 (Albert et al., 2006).

Those three *gamma-ray binaries* are composed of a massive star (O or Be type) and a neutron star or black hole in a ≈ 4 days (LS 5039), 26 days (LS I +61°303) and 1237 days (PSR B1259-63) eccentric orbit. Their TeV emission is at a level $\sim 10^{33-34}$ erg s^{-1}, comparable to the X-rays. Remarkably, all have been detected in the radio, a feature otherwise shared by only a handful of high-mass X-ray binaries. Bar from periodic radio outbursts in LS I +61°303 and PSR B1259-63, very likely related to passage of the compact object through the dense equatorial wind of the B*e* companion (LS 5039 has a O9V companion – and no such outburst), the emission from the systems is surprisingly steady up to timescales of years. This contrasts with typical HMXBs. Their spectral energy distributions superpose well with each other, with a rising spectral luminosity from radio to 0.1-1 MeV, a flat spectrum up to $1-10$ GeV and a drop at TeV energies.

The spectral and temporal similarities between the three binaries detected in VHE γ-rays hint at a common scenario. In PSR B1259-63, the relativistic wind emitted by the young 48 ms pulsar is contained by the stellar wind. Particle acceleration at the termination shock leads to X-ray synchrotron emission and γ-ray inverse Compton emission with the star photons. The measured pulsar spindown power is a modest $8 \cdot 10^{35}$ erg s^{-1}, implying rotation-power is converted into radiation with a high efficiency. The same scenario could be at work in LS 5039 and LS I +61°303 (Maraschi & Treves, 1981), explaining the spectrum, level and stability of the emission while uniting these sources in a new class of compact plerions (Dubus, 2006a). Pulsed radio emission would be strongly absorbed by the dense stellar wind in LS 5039 and LS I +61°303, with free-free opacities $\tau \gtrsim 10^3$. The pulse does vanish in PSR B1259-63 around periastron, when the pulsar probes the densest region of the Be wind.

2 High energy emission from a compact PWN

After the termination shock, a a pulsar wind nebula (PWN) of accelerated particles forms in the direction opposite to the apparent motion. The main properties are set by the distance of the shock R_S from the pulsar.

[1] Laboratoire Leprince-Ringuet, UMR 7638 CNRS/IN2P3/Ecole Polytechnique, F-91128 Palaiseau, France
Institut d'Astrophysique de Paris, UMR 7095 CNRS/UPMC Paris 6, 98bis boulevard Arago, F-75013 Paris, France

© Société Francaise d'Astronomie et d'Astrophysique (SF2A) 2006

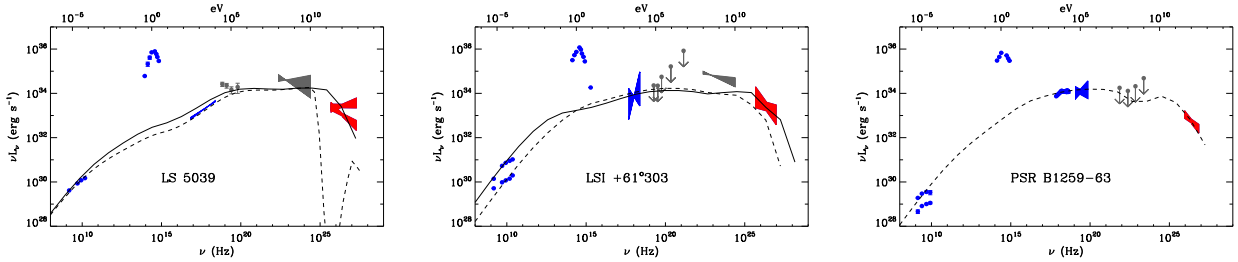

Fig. 1. Spectral energy distributions for the γ-ray binaries with PWN emission models. For LS 5039, the pulsar wind has $\dot{E}$=10^{36} erg/s, γ_w=5 10^4, σ=0.01, R_s=4 10^{11} cm at apastron (solid line) and 2 10^{11} cm at periastron (dashed line). The plot includes VHE $\gamma\gamma$ absorption (Fig. 2) but does not include emission from an associated cascade. For LS I +61°303, $\dot{E}$=10^{36} erg/s, γ_w=5 10^4, R_s=2 10^{11} cm and σ=0.02 at periastron in the dense equatorial wind (dashed line), changing to R_s=4 10^{12} cm and σ=0.005 at apastron in the polar wind (solid line). For PSR B1259-63, only periastron is shown with R_s=10^{12} cm, $\dot{E}$=8 10^{35} erg/s, γ_w=4 10^5 and σ=0.005.

2.1 Emission model

The pulsar wind is assumed have properties comparable to those of PSR B1259-63, with a power $\approx 10^{36}$ erg s^{-1} in mono-energetic e^+e^- pairs of Lorentz factor $\gamma_w \approx 10^5$. The wind magnetic field in small so that the ratio of magnetic to kinetic energy density $\sigma \approx 10^{-2}$. For LS 5039, the wind mass-loss rate is $\approx 10^7$ M$_\odot$ yr^{-1} with a terminal velocity ≈ 2000 km s^{-1} so that ram pressure balance give $R_s \approx 1.5 \cdot 10^{11} d_{0.1} \dot{E}_{36}^{1/2}$ cm, where $d_{0.1} = 0.1$ AU is the orbital separation. MHD shock conditions then set B, flow speed, density etc. Particles are accelerated to a $dN \propto \gamma^{-2} d\gamma$ power-law up to the radiative loss energy. The synchrotron and Klein-Nishina (KN) inverse Compton (IC) emission on stellar photons are calculated. Particles cool as they move away from the pulsar; changes in flow conditions are given by a Bernouilli equation.

The major features of the spectral energy distribution derive from considerations on timescales. Synchrotron losses always dominate over IC at the highest energies since $\dot{\gamma}_{\rm S} \propto \gamma^2$ while $\dot{\gamma}_{\rm IC} \propto 1/\gamma$ in KN regime. IC dominates below $\gamma_{\rm brk} \approx 6 \cdot 10^6 \ (T_{\star,4} R_{\star,10})/(B_1 d_{0.1})$ where $\dot{\gamma}_{\rm S}$=$\dot{\gamma}_{\rm IC}$. Assuming continuous injection of electrons with γ^{-2} spectrum, the steady-state distribution is steepened above $\gamma_{\rm brk}$ to γ^{-3}. This produces a flat synchrotron spectrum (in νF_ν) above $\nu_{\rm S} \approx 750 \, (T_{\star,4} R_{\star,10}/d_{0.1})^2 \, / B_1$ keV. The KN IC spectrum above $h\nu_{\rm IC} \approx \gamma_{\rm brk} m_e c^2 \approx 4 \, (T_{\star,4} R_{\star,10}/d_{0.1}) \, / B_1$ TeV is then $\nu F_\nu \propto \nu^{-1.5}$ (Moderski et al., 2005) . Below $\gamma_{\rm brk}$, inefficient KN losses dominate, producing a hard injection-like spectrum, hence a $\nu F_\nu \propto \nu^{0.5}$ synchrotron spectrum below $\nu_{\rm S}$ and a flat IC spectrum below $\nu_{\rm IC}$. Numerical SEDs for the three binaries are shown in Fig. 1, consistent with the above expectations.

2.2 Periodicities in LS 5039 and LS I +61°303

The evolution of the SED with orbital phase is straightforward: with a steady stellar wind along the orbit, then $B \propto 1/R_s \propto 1/d$. Hence, the spectrum should be unchanged at TeV energies but the hard X-ray spectral break should move as $1/d$. In LS 5039, d varies only by a factor 2, so few changes are expected in the intrinsic SED. However, HESS reports that the TeV flux is strongly modulated on $P_{\rm orb}$. This is due to pair production of TeV photons with stellar photons leading to stable, periodic absorption. Maximum flux occurs at inferior conjunction (ϕ=0.7, Fig. 2 and Dubus 2006b), as observed by HESS.

The source is never fully absorbed: VHE absorption must initiate a cascade re-emitting γ-rays at lower energies. At high fluxes the TeV spectrum is flat with a break at ≈ 8 TeV, suggesting $\gamma_{\rm brk}$ changes strongly with phase. The geometry of the interaction region may play a crucial role here, notably the anisotropy between seed photon, electron and observer for IC. The high velocities can also cause Doppler (de)boosting effects. Alternatively, an additional component might produce this hard spectrum, perhaps hadronic: nuclei in the pulsar wind are probably necessary to have non-thermal acceleration.

MAGIC reports detecting LS I +61°303 at apastron but not at phases ϕ=0-0.1 where the pulsar is in front of the star *i.e.* when absorption is weakest (Fig. 2). The TeV variability in LS I +61°303 is more likely due to the *Be* star than to $\gamma\gamma$ absorption. Be stars have a slow, dense equatorial wind and a fast, polar wind. The equatorial wind extends up to $\sim 20 \, R_\star$ so that the pulsar plunges periodically through the dense material. This

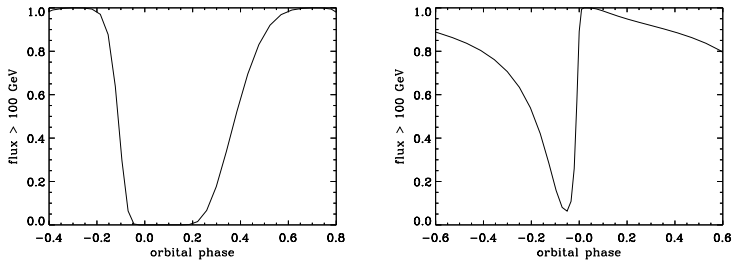

Fig. 2. Expected modulation of the >100 GeV flux due to $\gamma\gamma$ absorption in LS 5039 (left) and LS I +61°303 (right). Non-zero TeV fluxes are detected at ϕ=0-0.2 in LS 5039, probably due to cascading. For LS I +61°303, MAGIC detects the source at ϕ=0.3-0.5 but sees no flux at phases 0-0.1 despite little absorption. The variability is more likely to be intrinsic. (Note that periastron is often defined set at ϕ=0.23 instead of ϕ=0 in LS I +61°303.)

crushes the PWN, like the Earth magnetosphere during a Solar storm. R_s is close to the pulsar so B is high, $\nu_{\rm IC}$ is low and the steep IC spectrum leads to fainter TeV emission. At apastron the stellar wind is tenuous, R_s is further away from the pulsar so B is lower, $\gamma_{\rm brk}$ higher and IC emission more important at TeV, just as observed by MAGIC.

3 Radio tails

The radio emission in LS I +61°303 and LS 5039 has been resolved on angular scales of 10-100 mas and interpreted as due to relativistic jet emission by analogy with compact jets in X-ray binaries. The one-sidedness of the radio emission in LS 5039 was interpreted as a Doppler effect, implying a jet speed of $\approx c/3$. Strong changes in the orientation of the (one-sided) radio emission in LS I +61°303 on a timescale $\ll P_{\rm orb}$ were interpreted as jet precession. On larger scales, the radio emission appears to be more double-sided in LS 5039 and stable.

Emission from cooled PWN particles can explain the resolved radio fluxes very well. Isolated ms pulsars interacting with the ISM are known to emit well-collimated cometary tails of cooling shocked material in the direction opposite to motion, extending to parsec scales. Furthermore, colliding winds in some Wolf-Rayet binaries produce non-thermal radio emission whose appearance changes with orbital phase. In a γ-ray binary, the appearance of the PWN will combine the effects of cooling in a comet tail whose direction is changing with the pulsar's orbital motion. The aspect depends on orbital elements, shock geometry and cooling physics. For a face-on system (i=0°), the orbital motion creates a spiral with a step $\sim \sigma c P_{\rm orb}$, decreasing in intensity with distance. When the spiral is seen edge-on (i=90°), the PWN has a double-sided, jet-like aspect. Inclination effects are less pronounced in a highly eccentric system, which has a clear preferred direction for most of the orbit, with dramatic changes in the position angle of the tail around periastron (as seen in LS I +61°303 ?).

The PWN model predicts that the radio morphology at resolution $\sim \sigma c P_{\rm orb}$ should change on the orbital period. Maps at such resolutions depend mostly on geometric orbital effects and less on details of cooling. The milliarcsecond LS 5039 map close to periastron is in excellent agreement with the published VLBI map (Fig. 3). At resolutions $\gg \sigma c P_{\rm orb}$ the appearance is due to the summed emission of particles over many orbits (spiral steps), so the emission will be stable in morphology and intensity. Good knowledge of particle cooling and flow conditions are then required to make robust predictions at low resolutions.

4 Conclusion

Emission from a compact plerion provides a common, coherent framework to understand γ-ray binaries. These sources are the short-lived progenitors of accretion-powered HMXBs, which have slowly-rotating spundown pulsars. About 30 such sources are expected in our Galaxy given the present-day HMXB population (Meurs & van den Heuvel, 1989), consistent with seeing 3 within 3 kpc.

High-energy emission occurs on small scales. Strong variations in the location of the pulsar wind termination shock (LS I +61°303, PSR B1259-63) and $\gamma\gamma$ absorption of VHE photons on starlight (LS 5039) can cause periodic changes at X-rays energies and above. Particles leave the vicinity of the pulsar as they cool, forming

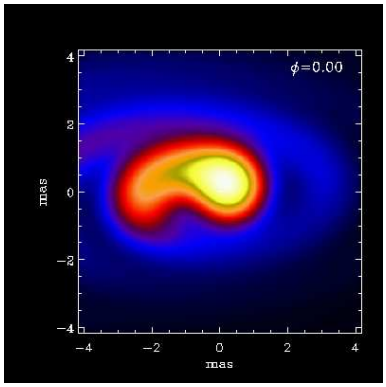

Fig. 3. Radio appearance of the PWN nebula of LS 5039 on mas scales at periastron. The basic shape is a spiral of decreasing intensity with a step $\sigma P_{\rm orb} c$ ($\approx$2 mas here with σ=0.01), projected on the sky with i=60°. The curved jet-like emission reproduces very well the only available VLBI observation (Paredes et al., 2000).

a cometary tail. Periodic changes in the aspect of this tail can be resolved in radio on scales $\sigma c P_{\rm orb}$, providing a test for the PWN scenario. The radio nebula is steady on larger scales.

Compact plerions enable access to pulsar wind physics on hitherto inaccessible scales. Detailed understanding of the VHE emission, notably in LS 5039, can provide important clues as to the shock geometry, magnetic field intensity and acceleration processes around young rotation-powered pulsars. Many of the new sources discovered by HESS in the Galactic plane appear to be associated with plerionic supernova remnants (SNR), of which γ-ray binaries may be only one particular kind. They might even be joined by the Galactic center TeV source, whose emission has been variously attributed to dark matter, the Sgr A* black hole or the Sgr A East SNR. There is also a plerion-like X-ray nebula within the HESS error box with the right properties to explain the VHE emission (Wang et al., 2006). Plerions are indeed the new stars of the VHE sky.

References

Aharonian, F. A., et al. (HESS collaboration) 2006, astro-ph/0607192
Aharonian, F. A., et al. (HESS collaboration) 2005a, Science, 309, 746
Aharonian, F. A., et al. (HESS collaboration) 2005b, A&A, 442, 1
Albert, J., et al. (MAGIC collaboration) 2006, Science, 312, 1771
Dubus, G. 2006a, A&A, in press (astro-ph/0605287)
Dubus, G., 2006b, A&A, 451, 9
Gotthelf, E. V. 2003, ApJ, 591, 361
Maraschi, L., & Treves, A. 1981, MNRAS, 194, 1P
Meurs, E. J. A., & van den Heuvel, E. P. J. 1989, A&A, 226, 88
Moderski, R. et al. 2005, MNRAS, 845
Paredes, J. M. et al. 2000, Science, 288, 2340
Wang, Q. D., Lu, F. J., & Gotthelf, E. V. 2006, MNRAS, 367, 937